iScience

CellPress

Article

One-Step Direct Fixation of Atmospheric CO_2 by Si-H Surface in Solution

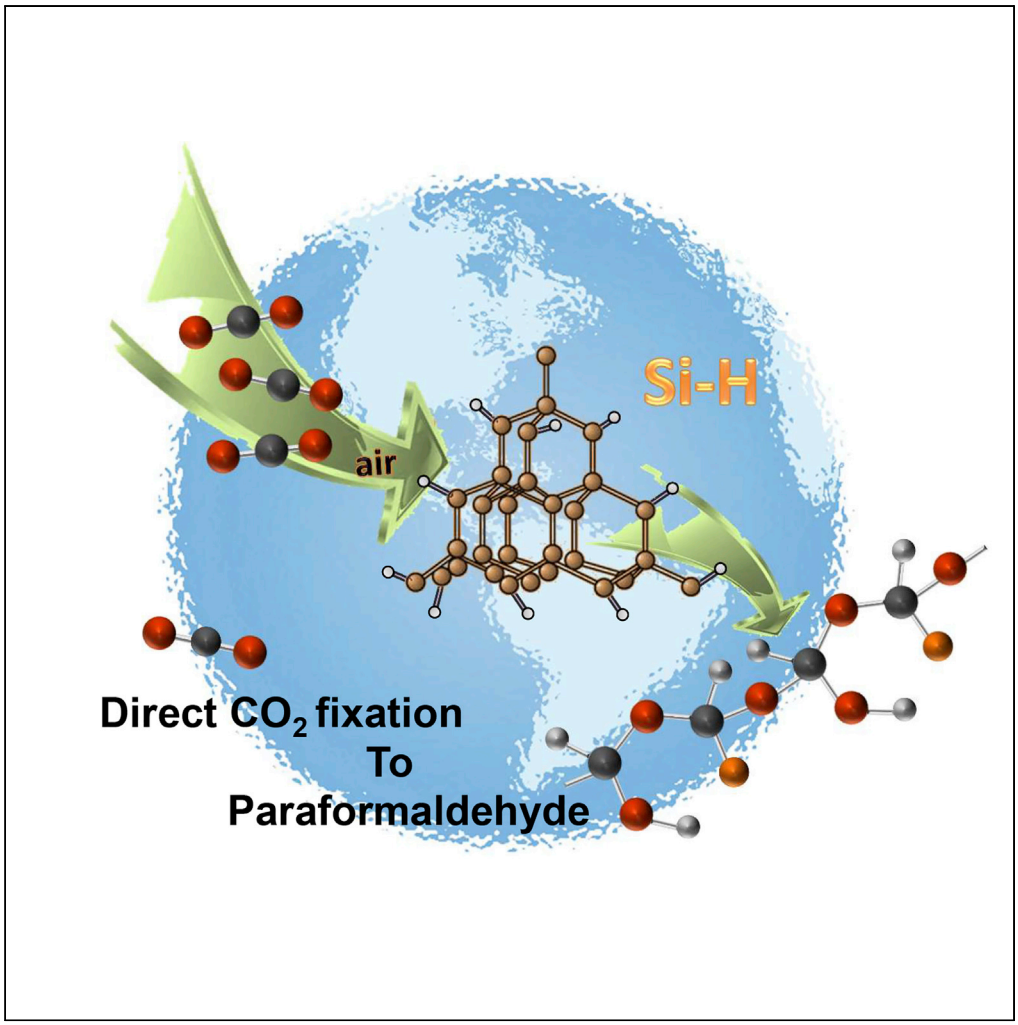

Zhenglong Fan, Fan Liao, Huixian Shi, Yang Liu, Qian Dang, Mingwang Shao, Zhenhui Kang

yangl@suda.edu.cn (Y.L.)
mwshao@suda.edu.cn (M.S.)
zhkang@suda.edu.cn (Z.K.)

HIGHLIGHTS

Atmospheric CO_2 is fixed with HF-treated silicon powders via one-step method

The product is fluorine substituted polymer (F-POM)

The fixation process is monitored by *in situ* infrared studies and mass spectra

The mechanism on the direct CO_2 fixation by Si-H surface is proposed

Fan et al., iScience *23*, 100806
January 24, 2020
https://doi.org/10.1016/j.isci.2019.100806

iScience

CellPress

Article

One-Step Direct Fixation of Atmospheric CO_2 by Si-H Surface in Solution

Zhenglong Fan,[1,2] Fan Liao,[1,2] Huixian Shi,[1] Yang Liu,[1,*] Qian Dang,[1] Mingwang Shao,[1,3,*] and Zhenhui Kang[1,*]

SUMMARY

The efficient conversion of carbon dioxide (CO_2) into useful chemicals has important practical significance for environmental protection. Until now, direct fixation of atmospheric CO_2 needs first extraction from the atmosphere, an energy-intensive process. Silicon (or Si-H surface), Earth-abundant, low-cost and non-toxic, is a promising material for heterogeneous CO_2 chemical fixation. Here we report one-step fixing of CO_2 directly from the atmosphere to a paraformaldehyde-like polymer by Si-H surface at room temperature. With the assistance of HF, commercial silicon powder was used as a heterogeneous reducing agent, for converting gaseous CO_2 to a polymer of fluorine substituted polyoxymethylene and hydroxyl substituted polyoxymethylene alternating copolymer (F-POM). Making use of the Si-H surface toward the fixation of atmospheric gaseous CO_2 is a conceptually distinct and commercially interesting strategy for making useful chemicals and environmental protection.

INTRODUCTION

The utilization of fossil fuels leads to significant increase of CO_2 (gigaton per year) concentrations in the atmosphere, which is generally considered to be the main reason for global warming. Now, the focus of attention of the scientific and technological world is to take effective methods to deal with the serious situation (Gao et al., 2016; Haszeldine, 2009; McDonald et al., 2015; Rao et al., 2017). These methods include carbon capture (Haszeldine, 2009), sequestration, and/or utilization (Gao et al., 2016; Rao et al., 2017). Among them, the conversion of CO_2 into valuable chemicals is considered as one of the most favorite ones, such as methanol (Graciani et al., 2014) and carboxylic acid (Banerjee et al., 2016). And the syntheses of urea, methanol, salicylic acid, synthetic gas, and organic carbonates have been industrialized.

Yet, the utilization of CO_2 is far from sufficient. There still remains a challenge for CO_2 fixation because CO_2 is thermodynamically stable (Gibbs free energy about −394.4 kJ/mol) and its activation has to break the strong C=O bonds with large bond energy of 532.2 kJ/mol (Luo, 2007) to further convert it into other value chemicals. Such activation can only be realized using active catalysts and additional energy input. The reactions associated with it are usually endothermic and have a positive change of enthalpy. In addition, direct fixation of atmospheric CO_2 needs to extract it from the atmosphere first; this process needs much energy (Bhanage and Arai, 2014). The values of the fixation products still need to improve (Clark et al., 2018). In this field, it is a huge challenge and requires an effective strategy to direct fixation of atmospheric CO_2 with one step at mild reaction conditions.

Heterogeneous catalytic fixation of CO_2 is one of the few approaches that have the potential to achieve this impressive feat, but it will require huge amounts of catalysts to facilitate CO_2 conversion on this grand scale. Therefore, the earth abundance, cost, and toxicity of the elements comprising the catalysts become determining factors for successful implementation of the process. Silicon would be one perfect choice on all the above three counts. Molecular silanes are known to convert CO_2 to its reduced forms (Schafer et al., 2012; Matsuo and Kawaguchi, 2006; Riduan et al., 2009; Berkefeld et al., 2010; Khandelwal and Wehmschulte, 2012). Recent studies have shown evidence that the hydrides of nanoscale Si materials are capable of reducing CO_2 (Qian et al., 2018; Sun et al., 2016). These demonstrations have explored the possibilities of CO_2 conversion using Si materials as the reducing agent, boasting a promising, low-cost solution to making value-added chemicals and fuels from CO_2 and high-energy inputs. However, it still requires a silicon-based strategy able to function at one-step direct fixation of atmospheric CO_2 by Si-H surface.

Here we report the direct fixation of CO_2 from the atmosphere to valuable chemical, fluorine substituted polyoxymethylene and hydroxyl substituted polyoxymethylene alternating copolymer (F-POM), by Si-H surface with the assistance of hydrofluoric acid at mild reaction conditions. In the present reaction system,

[1]Institute of Functional Nano & Soft Materials (FUNSOM), Jiangsu Key Laboratory for Carbon-Based Functional Materials & Devices, Soochow University, 199 Ren'ai Road, Suzhou, Jiangsu 215123, PR China

[2]These authors contributed equally

[3]Lead Contact

*Correspondence: yangl@suda.edu.cn (Y.L.), mwshao@suda.edu.cn (M.S.), zhkang@suda.edu.cn (Z.K.)

https://doi.org/10.1016/j.isci.2019.100806

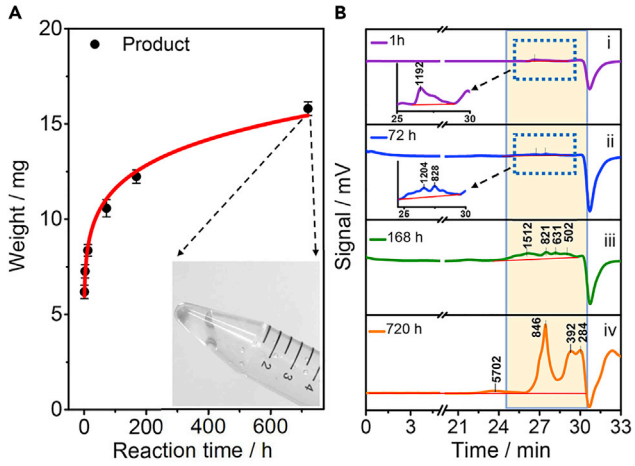

Figure 1. Direct Fixation of Atmospheric CO_2

(A) Time profile of the product yields. Data are mean of three individual experiments; the inset is an optical photograph of product with 720 h reaction time.

(B) GPC chromatogram of the as-prepared product (using ultra-pure water containing 0.1 mol/L sodium nitrate at rate of 1 mL/min as the solvent) with reaction times of 1, 72, 168, and 720 h, respectively; the inset is the enlarged view with time ranging from 25 to 30 min.

the reduction of CO_2 is mainly attributed to the high reductive ability of Si-H. For example, commercially available silicon powder (average diameter of 45 μm), with the assistance of HF, denoted Si-H surface continuously, can function as heterogeneous reducing agent for converting gaseous CO_2 to F-POM, at an initial rate of 6.24 mg·h^{-1}. With evidence from *in situ* infrared spectra and mass spectra, we acquired a clear and fundamental understanding on the direct fixation of atmospheric CO_2 by Si-H surface in HF solution. We further demonstrated that the industrial silicon is also available to directly fixing CO_2 from atmosphere into F-POM at normal temperature and pressure.

RESULTS

In our experiments, the silicon powder and 4 wt% HF solution were used to fix the atmospheric CO_2 in an open reaction system under ambient condition (Scheme S1). As shown in Figures S1A–S1C, the as-received silicon powder (10–80 μm) has a quasi-spherical shape with an average diameter of 45 μm. The phase and crystallography of the silicon powder are probed by the powder X-ray diffraction technique (Figure S1G). Typically, 200 mg silicon powder and 50 mL HF (4 wt%) solution were mixed into the container at ambient temperature in air. Air with CO_2 concentration of about 400 ppm was pumped into the 4 wt% HF aqueous solution with the volume flow rate of 1 L·min^{-1}. A series of experiments were carried out with the same material ratio (mole ratio of Si and HF is about 1:16) to study the product yield of this atmospheric CO_2 fixation reaction. After 1, 3, 12, 72, 168, and 720 h reaction time, the products (a viscous semi-solid, inset in Figure 1A) were collected with the amount of 6.24, 7.29, 8.29, 10.61, 12.19, and 15.89 mg, respectively. As shown in Figure 1A, the product yield increases with the extension of the reaction time at first and gradually tends to remain unchanged after 150 h. This feature indicates the products are formed from consumable solid reactant particles. In addition, the silicon powder after reaction was also characterized (Figures S1D–S1F). Furthermore, the conversion efficiency may be calculated from Table S2 in this revision and corresponding process would be written as $(W_{F\text{-}POM} \div M_{repeating\ unit\ of\ F\text{-}POM})/(W_{Si} \div M_{Si}) = (6.24 \times 10^{-6}\ kg \div 94\ kg/kmol)/(1.859 \times 10^{-5}\ kg \div 28\ kg/kmol) = 10\%$, which means it takes 10 moles of silicon to get one repeating unit of F-POM (or fix 2 moles of CO_2).

Next, we study this polymer-like product with various experimental techniques. Gel permeation chromatography (GPC) is applied to investigate the molecular weight distribution of the product (Figure 1B). Along with the reaction time the molecular weight of the polymer product increases. The varied peak positions show the increase process of the molecular weight. The main peaks (molecular weight) shaded by yellow area are located in range of 200–1,600. As shown in curve i, a low-molecular-weight peak appears at 1,192 when the reaction time is 1 h. The molecular weight of the product increases with reaction time; the highest molecular weights are 1,204 and 1,512 with reaction times of 72 and 168 h (curves ii and iii, respectively).

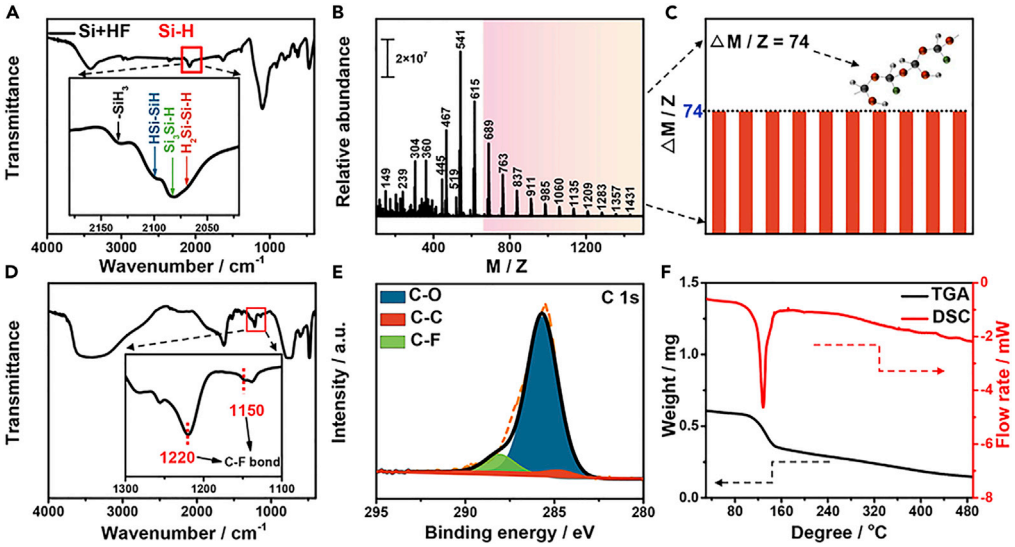

Figure 2. Characterization of Si-H Bond and F-POM Product with Reaction Time of 720 h

(A) FTIR of silicon powder with HF treatment; inset is the enlarged view with wavenumber ranging from 2,020 to 2,180 cm^{-1}.

(B) HRMS of the product. The products were directly injected into the MS instrument by means of an autosampler; there was no chromatographic separation step. The mass spectrometer was operated in the MRM mode with a positive ESI source.

(C) The histogram of differences between adjacent peaks.

(D) FTIR of the product; inset is the enlarged view with wavenumber ranging from 1,100 to 1,300 cm^{-1}, the peaks at 1,220 and 1,150 cm^{-1} corresponding to the characteristic peaks for C-F bonds.

(E and F) (E) XPS of C 1s for the product and (F) the curves of TGA (black curve) and DSC (red curve) of the product with heating rate of 10°C min^{-1} under air.

After 720 h reaction, the highest molecular weight of the product can reach up to 5,702, as shown in curve iv. The number-average molecular weight (M_n), weight-average molecular weight (M_w) and coefficient of dispersion Đ (Đ = M_z/M_w) of different peaks were determined using the GPC calibrations (see Table S1).

The Fourier transform infrared (FTIR) spectroscopy of HF-treated silicon powder (Figure 2A) and HF-treated silicon nanowires (Figures S1H–S1I) were collected, which clearly show their Si-H bonds (Sun et al., 2003; Yu et al., 2013). Electrospray ionization mass spectrometry (ESI-MS) full scan mass spectrum was further employed to determine the structure of the product. The high-resolution mass spectrum (HRMS) for product with reaction time of 720 h is shown in Figure 2B (the detailed data are shown in Figure S2). It is interesting to note that the differences between adjacent peaks are always 74 (Figure 2C), although there are numerous peaks. To further explain the origin of such a difference of m/z 74, an assumption is proposed that the product is a kind of polymer and the difference comes from its repeating unit. On the basis of ionization working mechanism, the repeating unit of the product is determined to be CH(OH)-O-CF-O (repeating unit of F-POM). In addition, control experiments were conducted using pure CO_2 and Ar as raw material to replace air. The corresponding MS result of the product obtained by pure CO_2 as raw materials is shown in Figure S3, which has the same differences between adjacent peaks of 74, similar to the data of product obtained by air as raw material. No product was obtained using Ar as raw material to replace air. These control experiments demonstrate that the final product was obtained from CO_2 instead of other molecules. Moreover, we conducted this experiment via using kerf silicon to replace industrial silicon powder. The as-received kerf silicon with average size of 17.5 μm is shown in Figure S4. In addition, the MS data are added as Figure S5, which showed similar results compared with data obtained by using industrial silicon powder as raw material. The differences between adjacent peaks (Δm/z) are also 74, which demonstrates the kerf silicon has features similar to that of industrial silicon powder; both can be used to fix carbon dioxide.

The FTIR spectrum shows two strong peaks at 1,220 and 1,150 cm^{-1} (Figure 2D), the characteristic ones for C-F bonds (Wang et al., 2016; Li et al., 2016). FTIR spectra of products with different reaction times

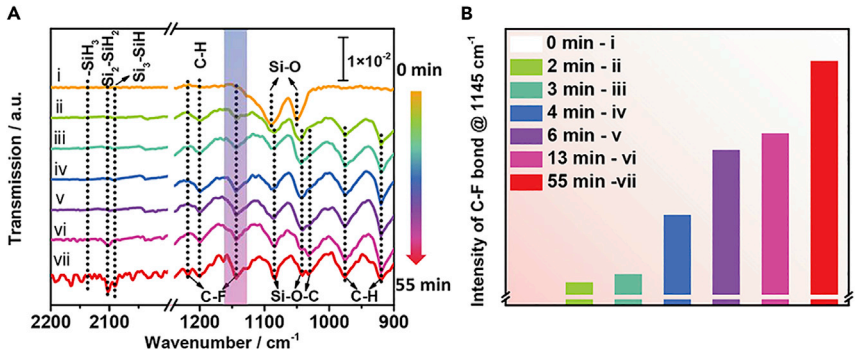

Figure 3. *In Situ* FTIR Analysis of the F-POM Formation

The reaction was conducted on a KBr micro-disk. Ten microliters HF (4 wt%) aqueous solution was added on 3 mg silicon powder in the KBr micro-disk.

(A) The FTIR spectra were extracted at different reaction times of (i) 0, (ii) 2, (iii) 3, (iv) 4, (v) 6, (vi) 13, and (vii) 55 min.

(B) The histogram of intensity of C-F bond at 1,145 cm^{-1} with change of time.

(Figure S6) indicate that the polymer is a fluoro one. For the purpose of further investigating the composition and corresponding valence states, the X-ray photoelectron spectroscopy (XPS) spectra of products with different reaction times were collected (Figures 2E and S7–S10). The high-resolution C 1s spectrum of product with reaction time of 720 h is shown in Figure 2E. The peaks at 284.6 and 286.0 eV were attributed to C-C and C-O bonds, respectively (Zhang et al., 2017). Notably, the peak at 288.2 eV is assigned to C-F bond. The corresponding peak at 685.8 eV in F 1s spectrum (Figure S7C) can further prove the presence of C-F bond (Feng et al., 2016; Wang et al., 2012), which is also consistent with FTIR analysis. In addition, the XPS spectra of products with reaction time of 1, 72, and 168 h were collected as well (Figures S8–S10), which show similar results with reaction time of 720 h.

To further better understand the information of thermodynamic properties for F-POM, the thermogravimetric analysis (TGA) and differential scanning calorimeter (DSC) with heating rate of 10°C min^{-1} were applied in air atmosphere (Figure 2F). It shows an obvious melting point with part decomposition at 132°C, similar with the thermogravimetric behavior of paraformaldehydes (Figure S11), which have the point in the range of 120°C –170°C, varying with their degree of polymerization. The TGA curve (Figure 2F) indicates that the product was a paraformaldehyde-like polymer with low degree of polymerization.

In addition, the TG-MS spectra of F-POM were shown in Figure S12. Along with the increasing temperature, five curves can be observed at M/Z = 18, 19, 30, 42, and 44 (Figure S12B). M/Z = 18 is attributed to H_2O; M/Z = 19 can be assigned to F ions; M/Z = 42 represents HC-O-CH fragment, and M/Z = 44 is determined to be CO_2. In addition, a difference value of 14 was observed in Figures S12C–S12E, respectively, which can be attributed to -CH_2 fragment. As CO_2 is the only carbon source for F-POM, the TG-MS result further proves atmospheric CO_2 can be directly fixed by Si-H in solution.

Finally, the GC-MS spectra of F-POM were shown in Figure S13. The result of GC-MS is a little different from that of ESI-MS owing to the different detection method. In brief, the detection method of GC-MS needs relatively high temperature, which makes it hard to obtain high-molecular weight fragment owing to direct decomposition of product. Three main peaks were observed in the MS spectrum (Figure S13). The peak at 57 can be assigned to the main chain of CH-O-C-O, and the difference value between 57, 71, and 85 is determined to be 14, which can be attributed to -CH_2.

To obtain insight on the formation of C-F bonds in the products, the CO_2 fixation reaction was conducted on a KBr micro-disk, located in the FTIR spectrometer, with the concentration of CO_2 maintained at 3,500 ppm (for details see Transparent Methods). The corresponding FTIR spectra were collected at different times (Figure 3A). At first, there is only silicon powder and only two strong Si-O peaks at 1,050 and 1,090 cm^{-1}. After the addition of HF solution and exposure of the silicon to CO_2 atmosphere, these two Si-O peaks disappear gradually and various new peaks appear; the peaks at 1,145 and 1,218 cm^{-1} belong to C-F bonds (Wang et al., 2016; Li et al., 2016); those at 1,030, 1,042 and 1,084 cm^{-1} are attributed to Si-O-C bonds (Schwartz et al., 2006; Jung and Park, 2011); and peaks at 920, 975, and 1,200 cm^{-1} are assigned to

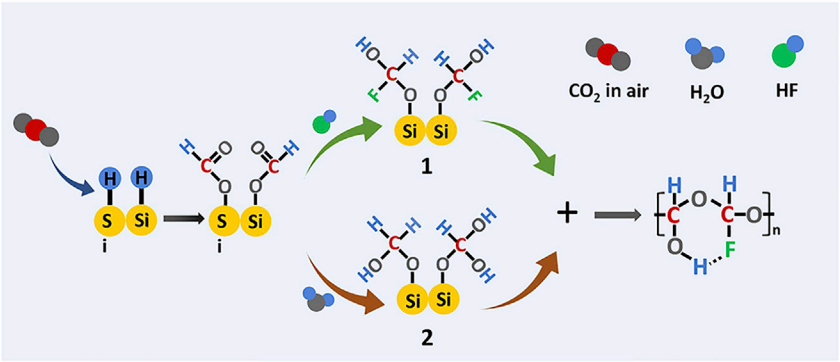

Scheme 1. Reaction Mechanism of the Direct Fixation of Atmospheric CO_2 by Si-H Surface in Solution
Numbers 1 and 2 indicate two reaction intermediates that can polymerize to the final F-POM product.

C-H bonds. With the increase of time, the intensity of C-F vibration becomes stronger (Figure 3B), indicating increase in the F-POM product. Along with the formation and growth of the C-F bond, the peak intensity of the Si-H bond becomes stronger as time goes on. The peaks at 2,090, 2,102, and 2,137 cm^{-1} can be attributed to Si_3-SiH, Si_2-SiH_2, and -SiH_3 bonds (Sun et al., 2003; Yu et al., 2013), respectively. This *in situ* FTIR clearly shows the formation of Si-H and C-F bonds, which demonstrate that the direct fixation of CO_2 by Si-H surface is feasible.

DISCUSSION

On the basis of the above characterization, the direct fixation mechanism of atmospheric CO_2 is schematically illustrated in Scheme 1. The first step is the formation of Si-H bonds on the surface of silicon via the addition of HF aqueous solution to remove the outer oxide. At the same time CO_2 was adsorbed on the surface of silicon and inserted into Si-H bonds to obtained Si-O-C(=O)-H (Schafer et al., 2012; Michele et al., 2016). In the following step, Si-O bond can be broken under existence of excessive HF aqueous solution. Fluorination and hydration of the first C atom were performed and two intermediates were obtained. And then, the product is formed via polymerization between those two intermediates. It is worth noting that the final product can be continually formed due to the existence of Si-H bond. The proposed mechanism has been listed as Note 2 in the Supplemental Information.

As shown in the above results, in the present reaction system, the reduction and fixing of CO_2 is mainly attributed to the high reductive ability of Si-H. After reaction, the Si-H surface can be regenerated with the assistance of HF, and then this reaction was continued until the Si was consumed. Furthermore, nanosized silicon or porous silicon structure will provide a large-specific-area Si-H surface, accelerating the CO_2 fixing reaction. Although the high concentration and/or high partial pressure of CO_2 are favorable to the CO_2 fixing reaction, the separation and extraction of CO_2 from air still need extra energy. Thus, the direct fixation of CO_2 from the air proposed by the present method has obvious advantages in saving energy and simplifying the process. Of course, if we can further develop our reaction system so that it can couple with the CO_2 emissions in the present industry process, it will greatly improve the efficiency of CO_2 fixing reaction.

In addition, silicon nanostructures have very rich photochemical properties, and then the introduction of solar irradiation into our reaction system may further enhance the fixing ability of atmospheric CO_2. Finally, we want to point out that, with silicon as raw material, CO_2 in air can be captured and fixed in HF solution to form F-POM, in which, SiF_4 and/or H_2SiF_6 are by-products. In addition, the massive product of polysilicon production up to 227,000 tons in 2013 (From Wikipedia, nd, https://encyclopedia.thefreedictionary.com/Polycrystalline+silicon.). It is estimated that about half of the silicon becomes kerf loss silicon during the slicing and lapping processes. Therefore, kerf loss silicon is a cheap and abundant material (Transparent Methods) (Dhanaraj et al., 2010). Low-value kerf loss silicon is also available to directly fix CO_2 from atmosphere into F-POM. The by-products SiF_4 could be converted to Si from the pyrolysis at high temperatures either at atmospheric or at low pressure (Mexmain et al., 1983), which will make up for the shortcomings (HF acid as raw materials, SiF_4 as by-product) of the present reaction system. This work opens up a new avenue to deal with the greenhouse gas CO_2, which is of great significance both for the scientific and practical values.

In summary, we report fixing CO_2 directly from the atmosphere to valuable chemical F-POM by Si-H surface with the assistance of hydrofluoric acid at room temperature. The reduction and fixing of CO_2 is mainly attributed to the high reductive ability of Si-H. After reaction, the Si-H surface can be regenerated with the assistance of HF (4 wt%), and then this reaction was continued until the Si was consumed. In the present reaction system, CO_2 is fixed with HF together to from a polymer (F-POM) and silicon was converted into silicon fluoride as a renewable by-product. We further demonstrated that the low-value industrial silicon is also available to directly fix CO_2 from the atmosphere into F-POM at normal temperature and pressure. Making use of the Si-H surface toward the fixation of atmospheric gaseous CO_2 is a conceptually distinct and commercially interesting strategy for making useful chemicals and environmental protection. This work also indicates that the Si-H surface might be employed to assist other catalytic processes in CO_2 conversion.

Limitations of the Study

We designed a new reaction system to fix atmospheric CO_2 directly by Si-H surface in solution. Although we can obtain a paraformaldehyde-like polymer in ambient condition, the safety of HF should be a notable thing. In addition, the mechanism should be proved by more advanced methods. The limitation of this study will be taken into account in our further work.

METHODS

All methods can be found in the accompanying Transparent Methods supplemental file.

SUPPLEMENTAL INFORMATION

Supplemental Information can be found online at https://doi.org/10.1016/j.isci.2019.100806.

ACKNOWLEDGMENTS

This work is supported by Development Program of China (2017YFA0204800), the National Natural Science Foundation of China (51902217, 51725204, 21771132, 21471106, 51972216, 51821002), the Collaborative Innovation Center of Suzhou Nano Science and Technology, the Priority Academic Program Development of Jiangsu Higher Education Institutions (PAPD), and the 111 Project, Joint International Research Laboratory of Carbon-Based Functional Materials and Devices. We thank Prof. Yeshayahu Lifshitz of Israel Institute of Technology for the thorough discussion and Prof. Guangcheng Xi of Chinese Academy of Inspection and Quarantine for his help in the high-resolution mass spectrum detection.

AUTHOR CONTRIBUTIONS

Z.F. and F.L. contributed equally to the conception and planning of the project and performance of the experiments and co-wrote the manuscript. Z.K, M.S., and Y.L. provided overall guidance in experimental design, experimental planning, data analysis and interpretation, scientific discussions throughout the project, and manuscript writing. H.S. and Q.D. conducted some experiments. Correspondence and requests for materials should be addressed to Y.L. (yangl@suda.edu.cn) or M.S. (mwshao@suda.edu.cn) or Z.K (zhkang@suda.edu.cn).

DECLARATION OF INTERESTS

The authors declare no competing interests.

Received: September 4, 2019
Revised: November 15, 2019
Accepted: December 20, 2019
Published: January 24, 2020

REFERENCES

Banerjee, A., Dick, G.R., Yoshino, T., and Kanan, M.W. (2016). Carbon dioxide utilization via carbonate-promoted C-H carboxylation. Nature *531*, 215–219.

Berkefeld, A., Piers, W.E., and Parvez, M. (2010). Tandem frustrated Lewis pair/tris(pentafluorophenyl) borane-catalyzed deoxygenative hydrosilylation of carbon dioxide. J. Am. Chem. Soc. *132*, 10660–10661.

Bhanage, B.M., and Arai, M. (2014). Transformation and Utilization of Carbon Dioxide (Springer), p. 203.

Clark, E.L., Resasco, J., Landers, A., Lin, J., Chung, L.T., Walton, A., Hahn, C., Jaramillo, T.F., and Bell, A.T. (2018). Standards and protocols for data acquisition and reporting for studies of the electrochemical reduction of carbon dioxide. ACS Catal. *8*, 6560–6570.

Dhanaraj, G., Byrappa, K., Prasad, V., and Dudley, M. (2010). Springer handbook of crystal growth (Springer-Verlag Berlin Heidelberg), pp. 1719–1728.

Feng, W., Long, P., Feng, Y.Y., and Li, Y. (2016). Two-dimensional fluorinated graphene: synthesis, structures, properties and applications. Adv. Sci. *3*, 1500413.

Gao, S., Lin, Y., Jiao, X.C., Sun, Y.F., Luo, Q.Q., Zhang, W.H., Li, D.Q., Yang, J.L., and Xie, Y. (2016). Partially oxidized atomic cobalt layers for carbon dioxide electroreduction to liquid fuel. Nature *529*, 68–71.

Graciani, J., Mudiyanselage, K., Xu, F., Baber, A.E., Evans, J., Senanayake, S.D., Stacchiola, D.J., Liu, P., Hrbek, J., and Sanz, J.F. (2014). Highly active copper-ceria and copper-ceria-titania catalysts for methanol synthesis from CO_2. Science *345*, 546–550.

Haszeldine, R.S. (2009). Carbon capture and storage: how green can black be? Science *325*, 1647–1652.

Jung, I.K., and Park, Y.T. (2011). Melt copolymerization reactions between 1,3-Bis(diethylamino)tetramethyldisiloxane and aryldiol derivatives. Bull. Kor. Chem. Soc. *32*, 1303–1309.

Khandelwal, M., and Wehmschulte, R.J. (2012). Deoxygenative reduction of carbon dioxide to methane, toluene, and diphenylmethane with $[Et_2Al]^+$ as catalyst. Angew. Chem. Int. Ed. *51*, 7323–7326.

Li, B.Y., He, T.J., Wang, Z.M., Cheng, Z., Liu, Y., Chen, T., Lai, W.C., Wang, X., and Liu, X.Y. (2016). Chemical reactivity of C-F bonds attached to graphene with diamines depending on their nature and location. Phys. Chem. Chem. Phys. *18*, 17495–17505.

Luo, Y.R. (2007). Comprehensive Handbook of Chemical Bond Energies (CRC Press, Taylor & Frnacis Group), p. 342.

Matsuo, T., and Kawaguchi, H. (2006). From carbon dioxide to methane: homogeneous reduction of carbon dioxide with hydrosilanes catalyzed by zirconium-borane complexes. J. Am. Chem. Soc. *128*, 12362.

McDonald, T.M., Mason, J.A., Kong, X.Q., Bloch, E.D., Gygi, D., Dani, A., Crocella, V., Giordanino, F., Odoh, S.O., and Drisdell, W.S. (2015). Cooperative insertion of CO_2 in diamine-appended metal-organic frameworks. Nature *519*, 303–308.

Mexmain, J.M., Morvan, D., Bourdin, E., Amouroux, J., and Fauchais, P. (1983). Thermodynamic study of the ways of preparing silicon, and its application to the preparation of photovoltaic silicon by the plasma technique. Plasma Chem. Plasma Process. *3*, 393–420.

Michele, A., Angela, D., and Eugenio, Q. (2016). Reaction Mechanisms in Carbon Dioxide Conversion (Springer), p. 128.

Qian, C.X., Sun, W., Hung, D.L.H., Qiu, C.Y., Makaremi, M., Kumar, S.G.H., Wan, L.L., Ghoussoub, M., Wood, T.E., and Xia, M.K. (2018). Catalytic CO_2 reduction by palladium-decorated silicon–hydride nanosheets. Nat. Catal. *2*, 46–54.

Rao, H., Chemidt, L.C.S., Bonin, J., and Robert, M. (2017). Visible-light-driven methane formation from CO_2 with a molecular iron catalyst. Nature *548*, 74–77.

Riduan, S.N., Zhang, Y.G., and Ying, J.Y. (2009). Conversion of carbon dioxide into methanol with silanes over n-heterocyclic carbene catalysts. Angew. Chem. Int. Ed. *48*, 3322–3325.

Schafer, A., Saak, W., Hasse, D., and Muller, T. (2012). Silyl cation mediated conversion of CO_2 into benzoic acid, formic acid, and methanol. Angew. Chem. Int. Ed. *51*, 2981–2984.

Schwartz, M.P., Barlow, D.E., Russell, J.N., Weidkamp, K.P., Butler, J.E., D'Evelyn, M.P., and Hamers, R.J. (2006). Semiconductor surface-induced 1,3-hydrogen shift: the role of covalent vs zwitterionic character,. J. Am. Chem. Soc. *128*, 11054–11061.

Sun, X.H., Wang, S.D., Wong, N.B., Ma, D.D.D., Lee, S.T., and Teo, B.K. (2003). FTIR spectroscopic studies of the stabilities and reactivities of hydrogen-terminated surfaces of silicon nanowires. Inorg. Chem. *42*, 2398–2404.

Sun, W., Qian, C.X., He, L., Ghuman, K.K., Wong, A.P.Y., Jia, J., Jella, A.A., O'Brien, P.G., Reyes, L.M., Wood, T.E., et al. (2016). Heterogeneous reduction of carbon dioxide by hydride-terminated silicon nanocrystals. Nat. Commun. *7*, 12553.

Wang, Y., Lee, W.C., Manga, K.K., Ang, P.K., Lu, J., Liu, Y.P., Lim, C.T., and Loh, K.P. (2012). Fluorinated graphene for promoting neuro-induction of stem cells. Adv. Mater. *24*, 4285–4290.

Wang, X., Wang, W.M., Liu, Y., Ren, M.M., Xiao, H.N., and Liu, X.Y. (2016). Characterization of conformation and locations of C-F bonds in graphene derivative by polarized ATR-FTIR. Anal. Chem. *88*, 3926–3934.

From Wikipedia, the free encyclopedia. https://en.wikipedia.org/wiki/Polycrystalline_silicon.

Yu, Y.X., Hessel, C.M., Bogart, T.D., Panthani, M.G., Rasch, M.R., and Korgel, B.A. (2013). Room temperature hydrosilylation of silicon nanocrystals with bifunctional terminal alkenes. Langmuir *29*, 1533–1540.

Zhang, C.M., Zhao, M.H., Wang, L.B., Qu, L.J., and Men, Y.J. (2017). Surface modification of polyester fabrics by atmospheric-pressure air/He plasma for color strength and adhesion enhancement. Appl. Surf. Sci. *400*, 304–311.

ISCI, Volume *23*

Supplemental Information

One-Step Direct Fixation of Atmospheric CO_2 by Si-H Surface in Solution

Zhenglong Fan, Fan Liao, Huixian Shi, Yang Liu, Qian Dang, Mingwang Shao, and Zhenhui Kang

Supplemental Information

Supplemental figures

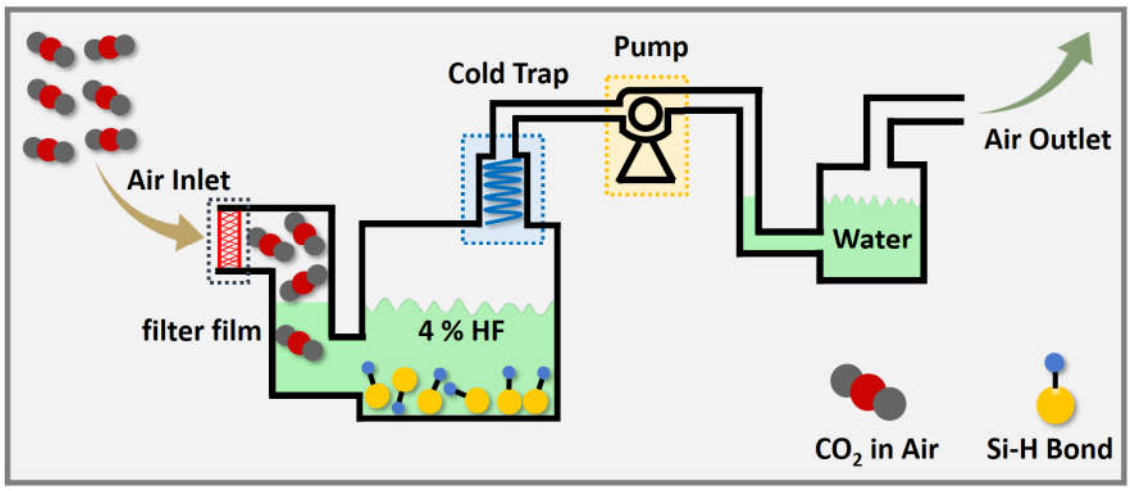

Scheme S1. The reaction device (Related to Figure 1). In this system, the CO_2 was from air and treated by filter film made of pottery with pore diameter of 1.2-2 μm, which go into device by mechanical pump. The unreacted HF can be reused via cold trap and absorption of water.

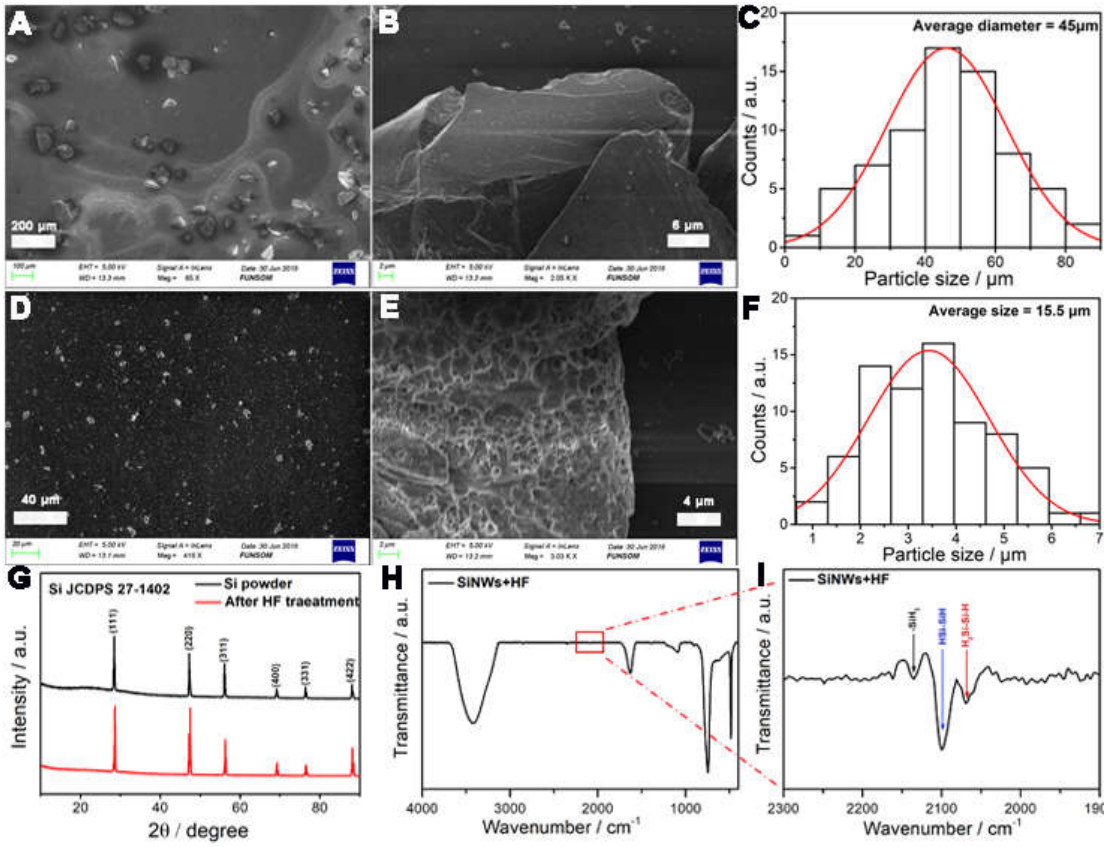

Figure S1. The characterization of raw silicon powder and silicon powder with HF treatment (Related to Figures 1 and 2). (**A**) SEM image of raw silicon powder, (**B**) enlarged view from (**A**); (**C**) corresponding histogram of particle size distribution for raw silicon powder, which show the average diameter is 45 μm; (**D**) SEM image of silicon powder with HF treatment; (**E**) enlarged view from (**D**); (**F**) corresponding histogram of particle size distribution for silicon powder with HF treatment, which show the average diameter is 15.5 μm; (**G**) XRD patterns of silicon powder before (black curve) and after HF treatment (red curve)**.** (**H**) FTIR of silicon nanowires (SiNWs) with HF treatment. (**I**) enlarged view for wavenumber ranging from 1900 to 2300 cm^{-1}.

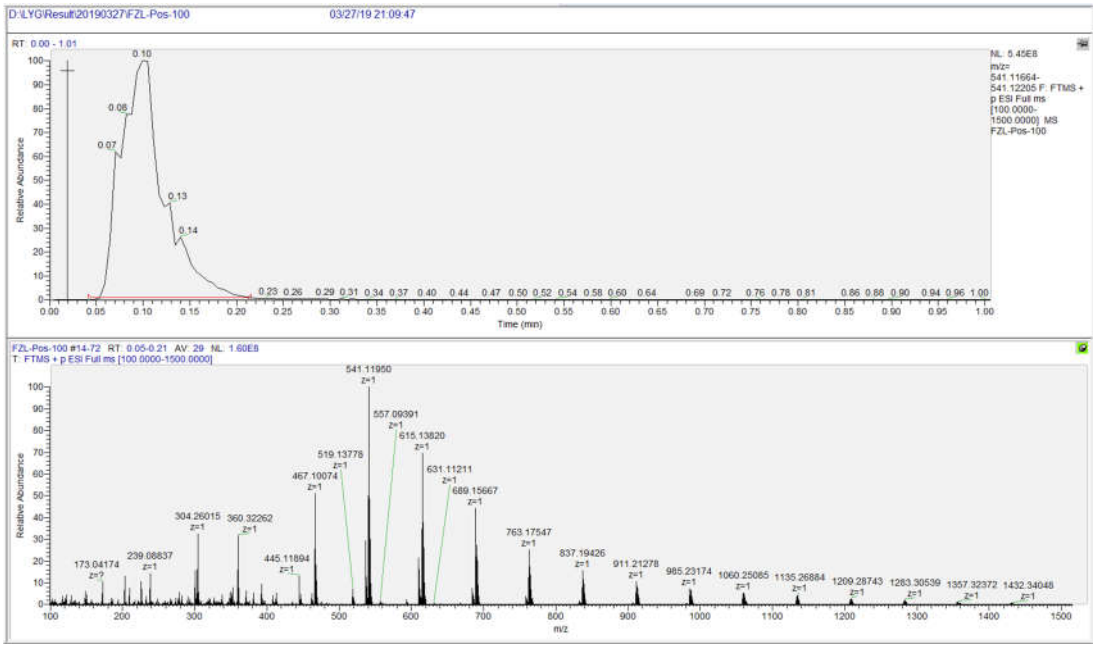

Figure S2. The original data of the HRMS spectra of products using air as raw material (Related to Figure 2). The product was directly injected into the MS instrument by an auto sampler without chromatographic separation step. The mass spectrometer was operated in the MRM mode with a positive ESI source.

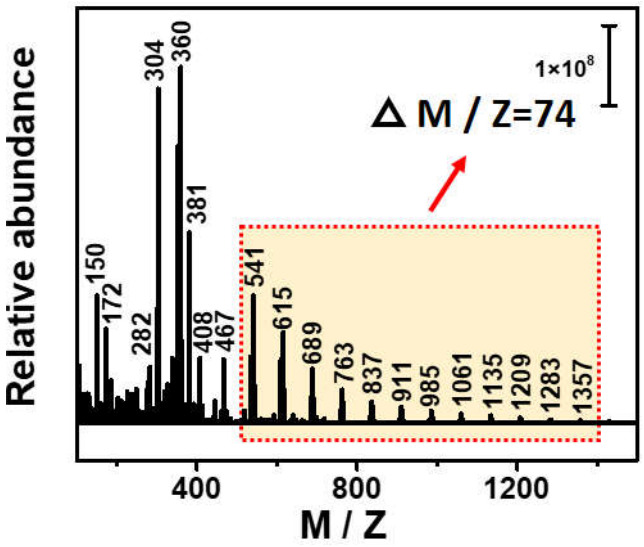

Figure S3. HRMS of the product using pure CO_2 as raw material (Related to Figure 2). The product was obtained via using pure CO_2 instead of air as raw material, which were directly injected into the MS instrument by an auto sampler without chromatographic separation step. The mass spectrometer was operated in the MRM mode with a positive ESI source.

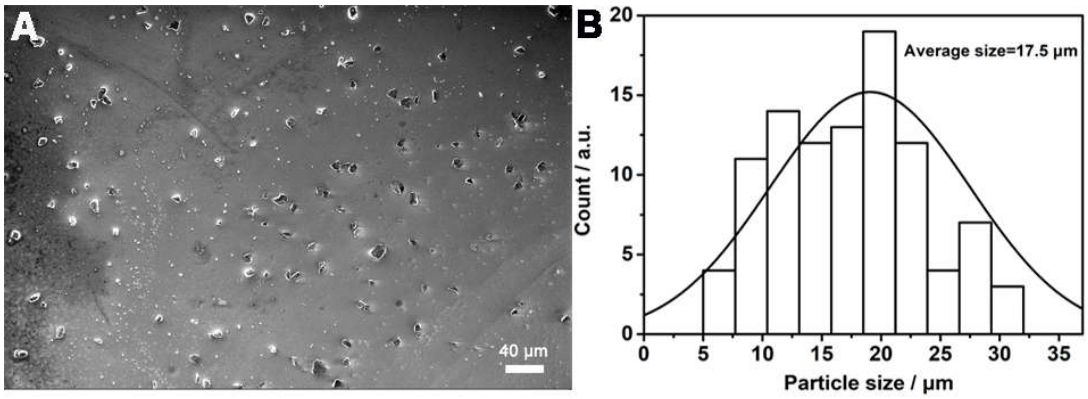

Figure S4. Morphology and size of kerf silicon (Related to Figure 2). (A) SEM image of raw kerf silicon; (B) corresponding histogram of particle size distribution for raw silicon powder, which show the average diameter is 17.5 μm.

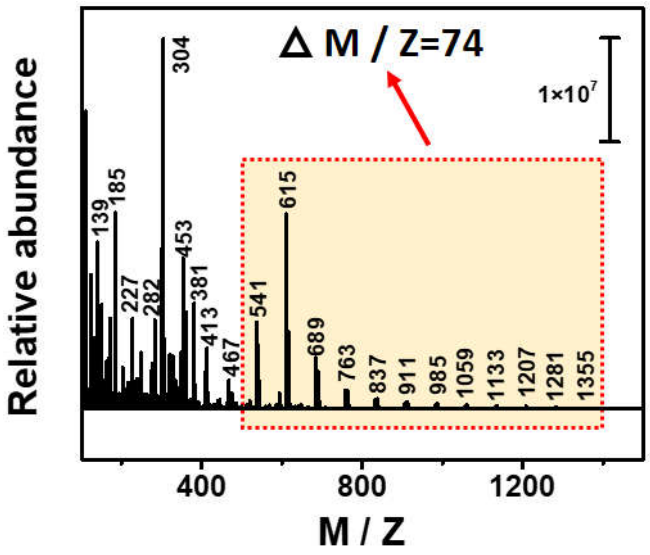

Figure S5. HRMS of the product using kerf silicon as raw material (Related to Figure 2). The product was obtained via using pure CO_2 instead of air as raw material, which were directly injected into the MS instrument by an auto sampler without chromatographic separation step. The mass spectrometer was operated in the MRM mode with a positive ESI source.

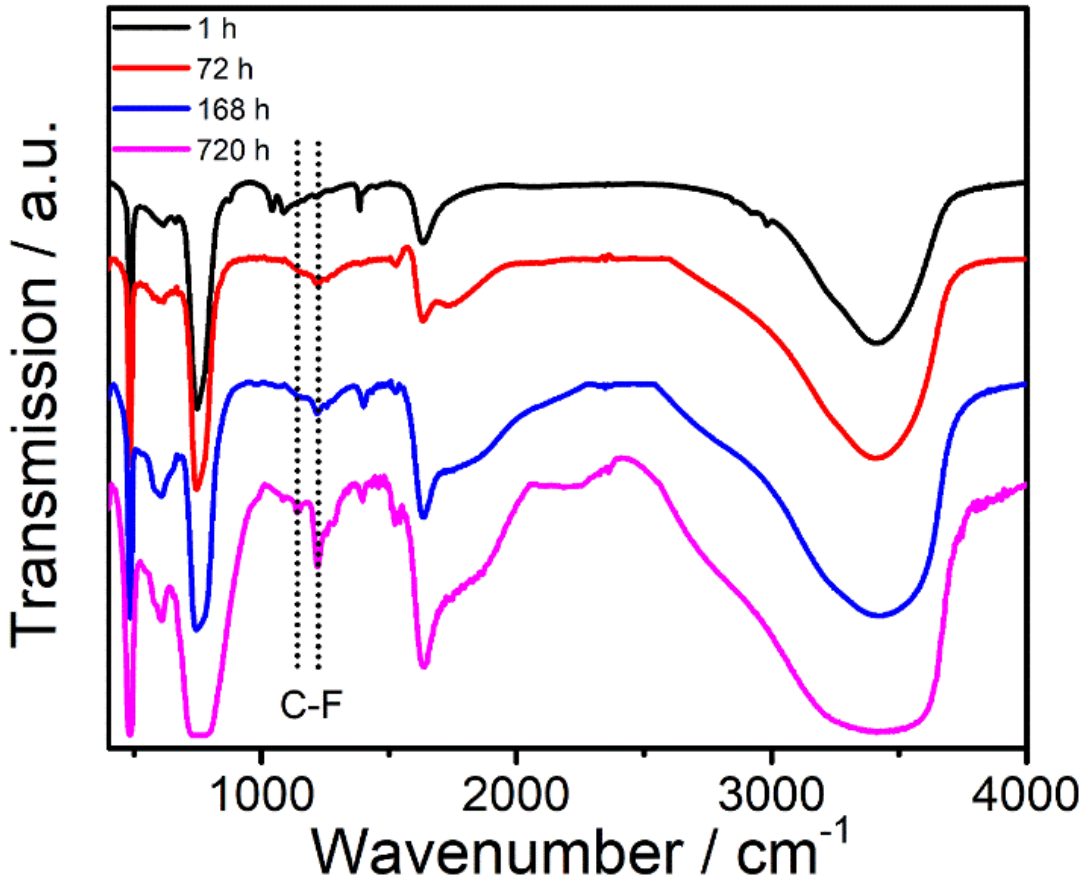

Figure S6. The FTIR of products with reaction time of 1, 72, 168 and 720 h (Related to Figure 2).

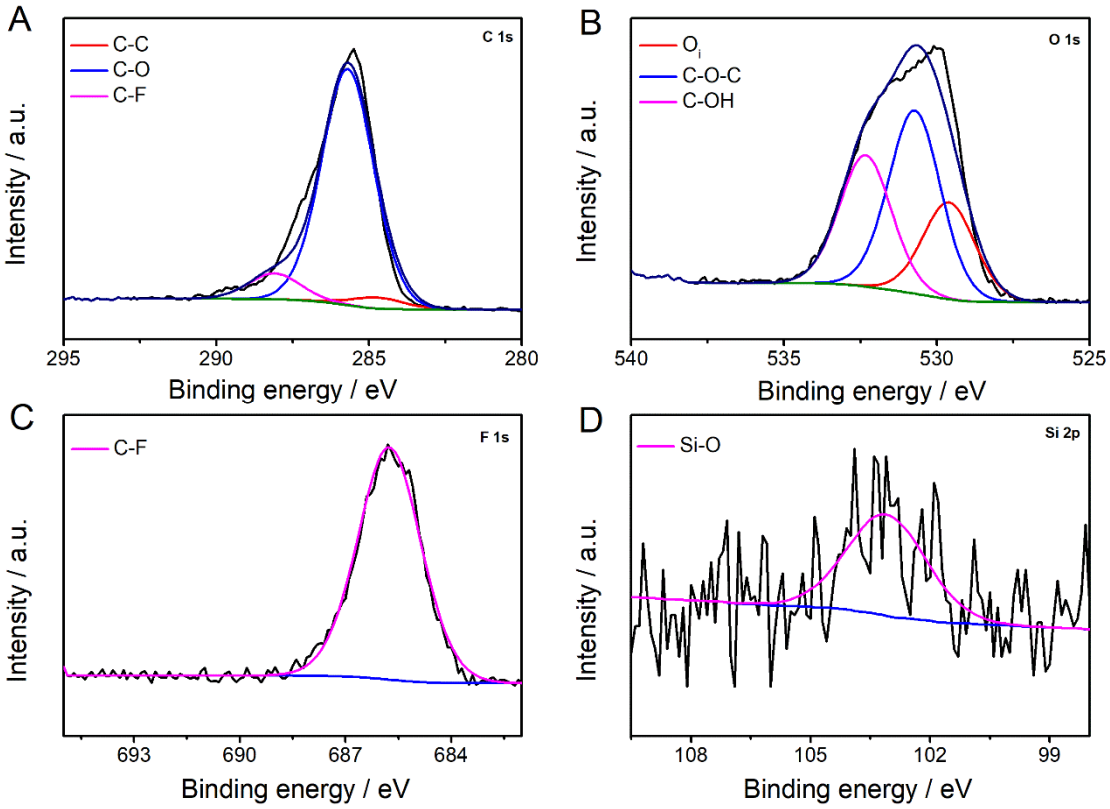

Figure S7. XPS spectra of product with reaction time of 720 h (Related to Figure 2). (**A**) full scan of product, (**B**) the high-resolution C 1s spectrum, (**C**) the high-resolution F 1s spectrum, and (**D**) the high-resolution O 1s spectrum.

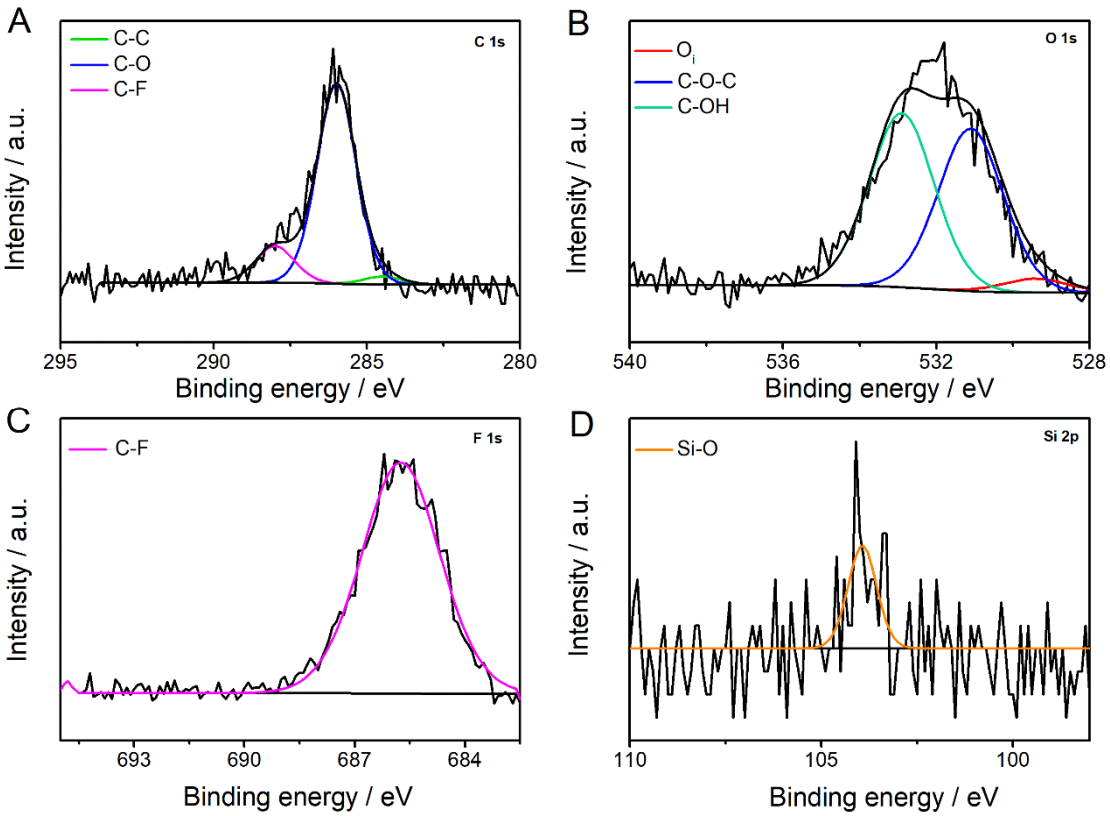

Figure S8. XPS spectra of product with reaction time of 1 h (Related to Figure 2). (**A**) the high-resolution C 1s spectrum, (**B**) the high-resolution F 1s spectrum, (**C**) the high-resolution O 1s spectrum, and (**D**) the high-resolution Si 2p spectrum.

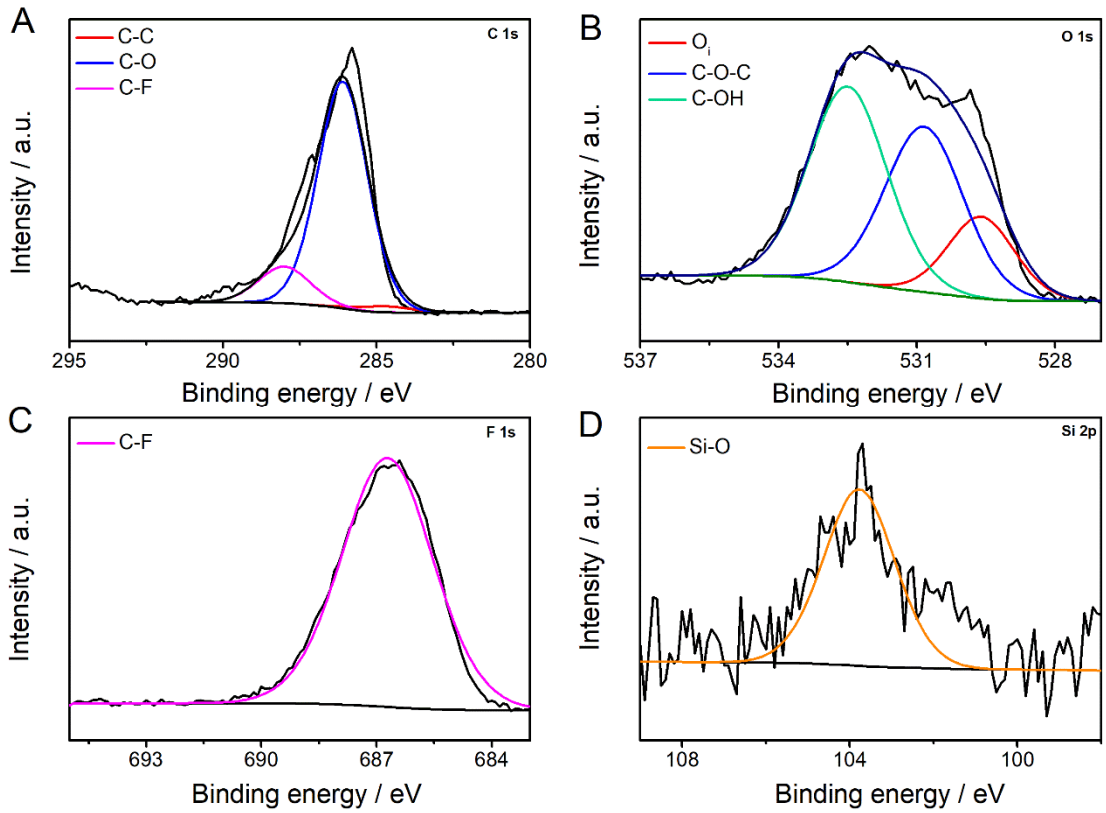

Figure S9. XPS spectra of product with reaction time of 72 h (Related to Figure 2). (**A**) the high-resolution C 1s spectrum, (**B**) the high-resolution F 1s spectrum, (**C**) the high-resolution O 1s spectrum, and (**D**) the high-resolution Si 2p spectrum.

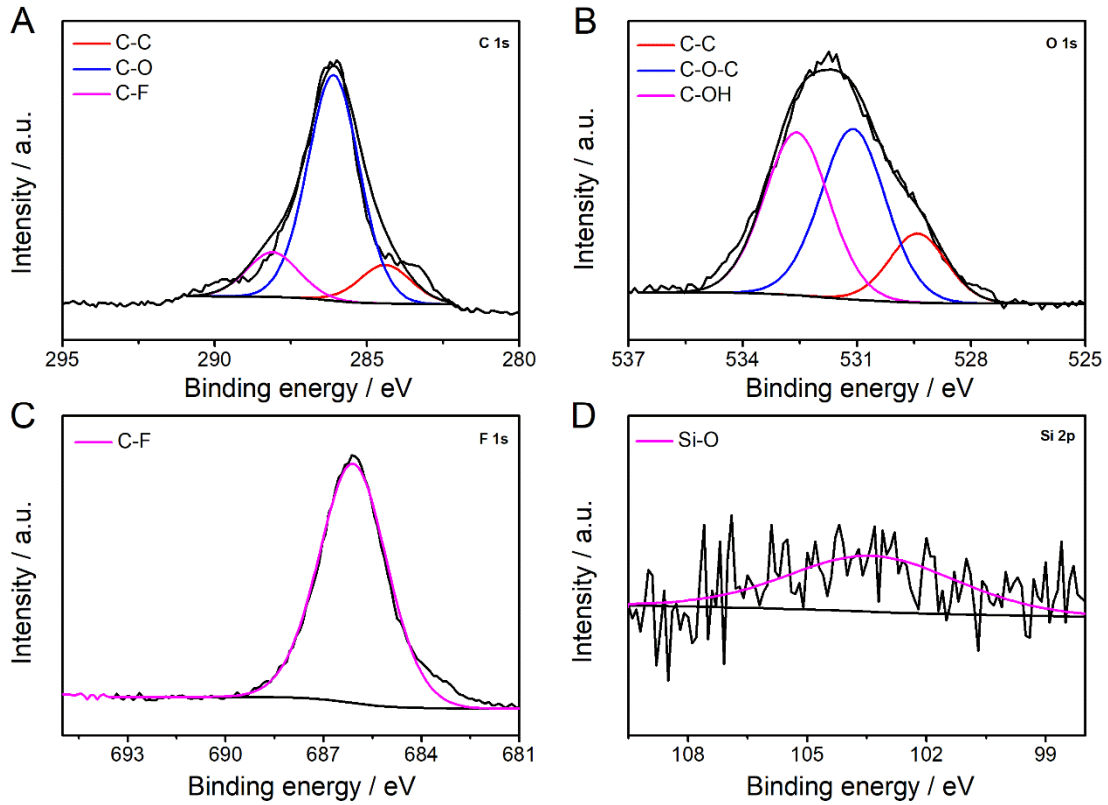

Figure S10. XPS spectra of product with reaction time of 168 h (Related to Figure 2). (**A**) the high-resolution C 1s spectrum, (**B**) the high-resolution F 1s spectrum, (**C**) the high-resolution O 1s spectrum, and (**D**) the high-resolution Si 2p spectrum.

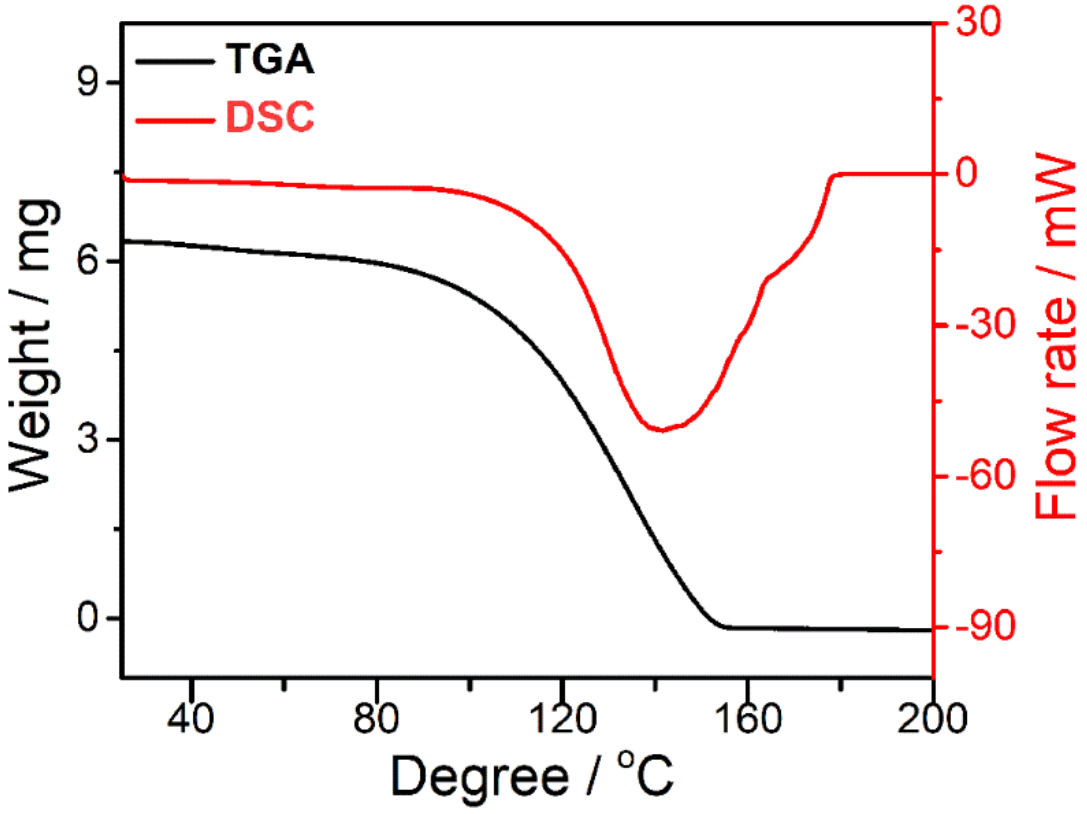

Figure S11. The TGA and DSC of paraformaldehyde (from J & K Chemical Corporation) (Related to Figure 2). The heating rate is 10 °C min^{-1} under air.

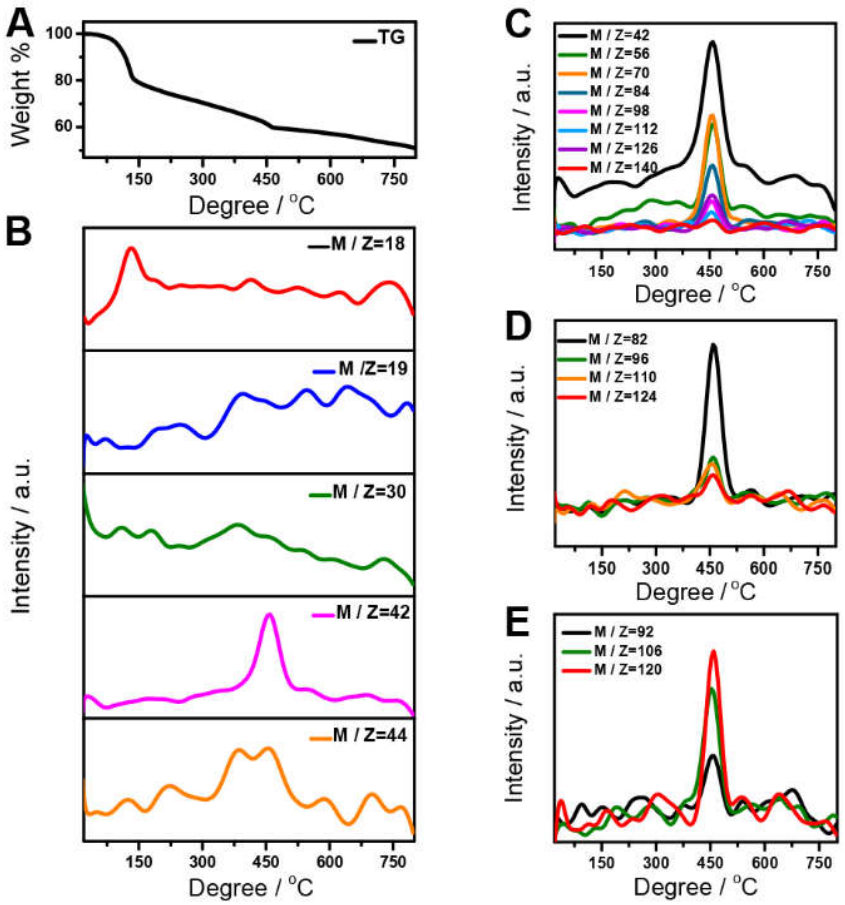

Figure S12. The TG-MS result of F-POM with heating rate of 10 °C min^{-1} under helium (Related to Figure 2). (A) The TG curve of F-POM, (B) MS curves for M/Z = 18, 19 30, 42 and 44 respectively; (C) the curves of M/Z = 42, 56, 70, 84, 98, 112, 126 and 140; (D) the curves of M/Z=82, 96, 110 and 124; and (E) the curves of M/Z=92, 106 and 120.

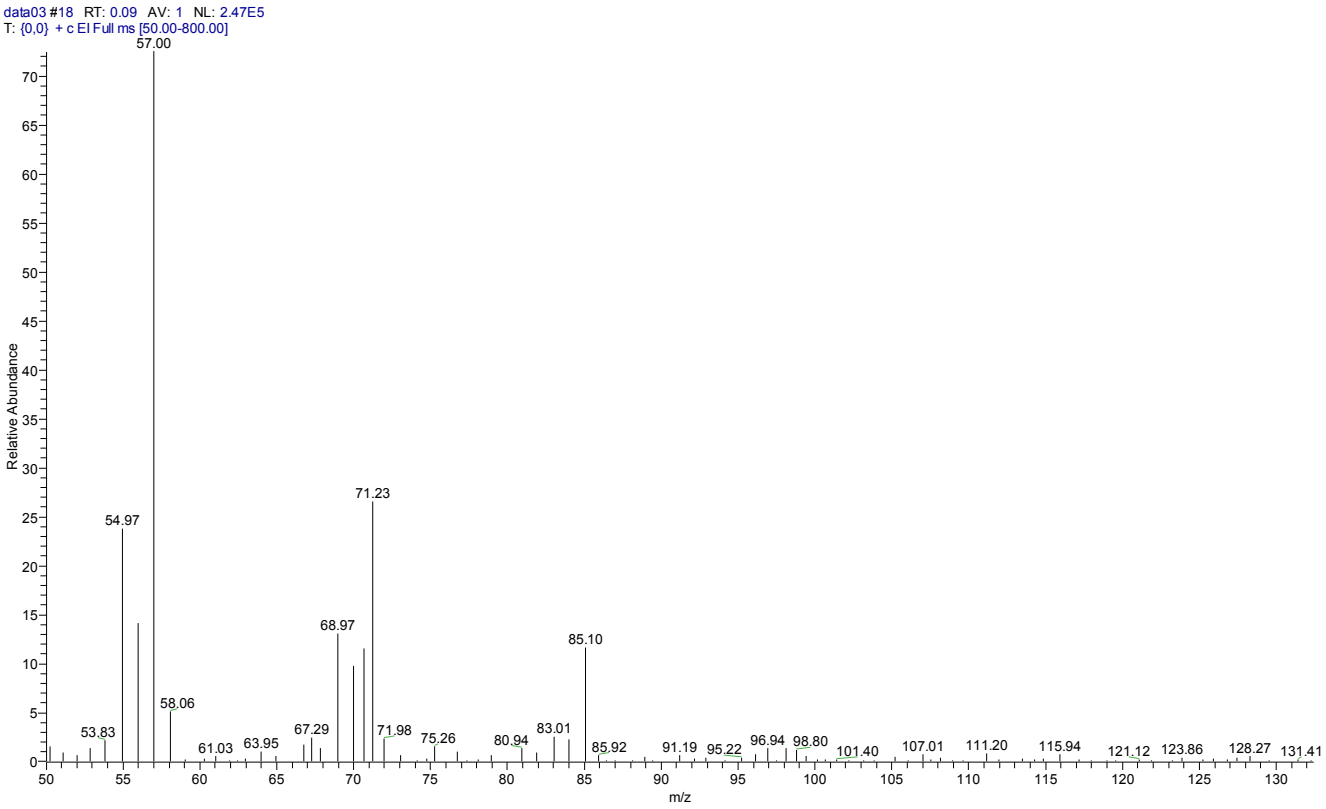

Figure S13. The GC-MS result of F-POM (Related to Figure 2). The product is tested via Trace ISQ with a direct injection method under helium atmosphere.

Supplemental tables

Table S1. GPC results for product with different reaction time (Related to Figure 1).

Time	Peak	Mn	Mw	MP	Mz	Mz/Mw	Area	Area%
1h	1	990	1028	1192	1064	1.034841	115512	100
72h	1	/	/	828	/	/	43825	40.3
	2	1434	1534	1204	1651	1.076101	64584	58.57
168h	1	1609	1794	1512	2023	1.127911	309000	51.25
	2	/	/	631	/	/	94250	15.63
	3	/	/	502	/	/	88880	14.74
	4	/	/	821	/	/	110743	18.38
720h	1	/	/	846	/	/	7613954	44.6
	2	/	/	392	/	/	5437059	31.85
	3	4761	5610	5702	6481	1.155363	503421	2.95
	4	/	/	284	/	/	3516371	20.6

Table S2. Cost analysis for whole experiment[a] (Related to Figure 1).

Raw materials	Cost	Dosage	Total price (10^{-4}×RMB ($))
HF[b]	1 RMB (0.14 $) / kg	6.638×10^{-5} kg	-0.7 (-0.1 $)
Kerf Silicon[c]	0.25 RMB (0.036 $) / kg	1.859×10^{-5} kg	-0.5 (-0.07 $)
Electricity	0.52 RMB (0.074 $)/ kWh	5×10^{-4} kWh	-26.0 (-3.71 $)
Product (F-POM)[d]	48 RMB (6.85 $)/ kg	6.24×10^{-6} kg	+29.9 (+4.27 $)

[a]These data were based on 1-hour reaction time.

[b]The price of HF (Industrial grade) was set by reference to Fujian Shanshui Chemical CORP.LTD.

[c]The price of Kerf silicon was set by reference to Tianneng Limited Company Changzhou Jiangsu.

[d]the price of F-POM was set by reference to the DuPont company (POM).

Table S3. The concentration of CO_2 for air inlet and air outlet (Related to Figure 1).

The concentration of CO_2 in air inlet	400 ppm
The concentration of CO_2 in air outlet	293 ppm

Table S4. The change of composition of air in air inlet and air outlet (Related to Figure 1)**.**

Composition	**CO_2**	**CO**	**N_2**	**O_2**
Change of composition	-107 ppm	N/A	N/A	N/A

Table S5. The change of amount of Si powder after 1h reaction (Related to Figure 1).

The amount of Si powder before reaction	200 mg
The amount of Si powder after reaction	181.4 mg

Transparent methods

1. Materials

Hydrofluoric acid (HF, 40 wt% analytical reagent) was bought from Sinopharm Chemical Reagent Corporation, which can be diluted to 4% by adding proportionable doubly-distilled water. Industrial silicon powder (the purity over 99%) was also supported by Sinopharm Chemical Reagent Corporation and the average diameter is 45 μm. In addition, kerf silicon was provided by Tianneng Limited Company Changzhou Jiangsu. Pure CO_2 was purchased from Baosteel Group Shanghai No.5 Steel Co., Ltd. and corresponding purity is 99.6%. Paraformaldehyde was obtained by J&K Chemical Technology Corporation. Other reagents were analytical reagent grade without further purification. Doubly-distilled water was used in all experiment.

2. Direct fixation of atmospheric CO_2 by Si-H surface in HF solution

First, 200 mg silicon powder and 50 mL HF (4 wt%) were added into a container and stirred for different times. The corresponding reaction device was illustrated in Figure 4. It is worth noting that the concentration of HF in the effluent gas is lower than the emission standard[S1] after absorption of water. In addition, the unreacted HF can be re-used via cold trap and water absorption. The HF was used to remove the outer oxide shell of silicon powder and form Si-H bonds on their surface. The CO_2 was captured by continuous stirring the above mixture in air. After a certain reaction time, the mixture was centrifuged and the filter liquor was dried with flowing air. All the experiments were performed in room temperature.

3. FTIR monitoring the reaction on a KBR micro-disk

First, 3 mg silicon powder was added into 50 mg KBr and grinded it for some minutes, then it was made into sample of FTIR. The first testing (the concentration of CO_2 is kept in 3500 ppm in whole testing process) was recorded as 0 minute, after first testing, the 10 μL (4 wt%) HF was added into sample, then data was recorded in 2, 4, 6, 10,20 and 55 mins, respectively.

4. Material Characterizations

X-ray powder diffraction (XRD, Philips X'pert PRO MPD diffractometer) with Cu Kα radiation source (λCu = 0.15406 nm) was used to research the phase and crystallography of the industrial silicon. The states of product was analyzed by using X-ray photoelectron spectroscopy (XPS) on a Kratos AXIS UltraDLD ultrahigh vacuum surface analysis system with Al Kα radiation (1486 eV) as a probe. Scanning electron microscopy (SEM) was carried out by using a Zeiss Gemini 500. FTIR (HYPERION Bruker) was used to Vibration of chemical bonds. Differential Scanning Calorimeter (DSC) was used to measure the melting point of the products via using DSC1 at a heating rate of 10 °C min^{-1} under air. Thermogravimetric analysis (TGA) was carried out by using a TA SDT 2960 instrument at a heating rate of 10 °C min^{-1} under air. All GPC data were obtained by using WATERS 1515, equipped with Waters 1515 Isocratic HPLC Pump and Waters 2414 Refractive Index Detector. The chromatographic separation was performed in ULTRAHYDROGEL 120 PKGD,

ULTRAHYDROGEL 250 PKGD and ULTRAHYDROGEL 500 PKGD columns and using Ultra-pure water containing 0.1 mol/L sodium nitrate at rate of 1 mL/min as the solvent. The high resolution mass spectrum (HRMS) of as-prepared product was collected by using Q Exactive Focus. The products were directly injected into the MS instrument by means of an autosampler with no chromatographic separation step. The mass spectrometer was operated in the MRM mode with a positive ESI source and the eluent was 100% water. The TG-MS spectra of product were obtained by Thermo Mass with heating rate of 10 °C min^{-1} under helium. The GC-MS result of product is tested via Trace ISQ with a direct injection method under helium atmosphere. The concentration of CO_2 was determined by carbon dioxide detector (UNI-T A37), which was placed in air inlet and air outlet and corresponding concentration can be shown on the screen.

5. Information for kerf loss silicon

Kerf losses for wiresaw and inner diameter saw are 180-210 μm and 300-500 μm, while the typical thicknesses of wafer for these slicing are 200 μm and 350 μm, respectively[26]. Therefore, kerf loss rate of output-to-input for wiresaw and inner diameter saw are in the ranging of 47.3-51.2% and 46.1-58.8%, respectively, which means that about half of the silicon becomes kerf loss during the silicon wafer production.

6. A possible polymerization mechanism

(1) Forming Si-H bonds on the surface of silicon powder

$$(Si_{bulk}\equiv Si)_3\equiv Si\text{-}OH + 4HF \longrightarrow 3Si_{bulk}\equiv Si\text{-}H + SiF_4 + H_2O$$

(2) Inserting CO_2

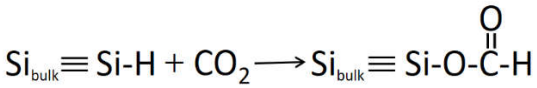

(3) Fluorination or hydration of the first C atom

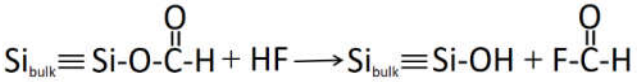

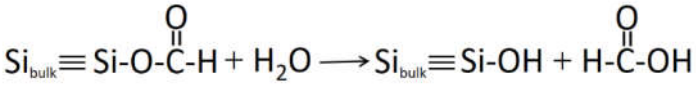

(4) Polymerization

1) Hemiacetal reaction

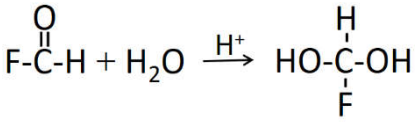

2) Hemiacetal reaction

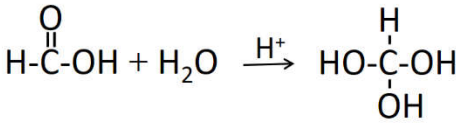

3) Alcohol dehydration to form ether in acid media

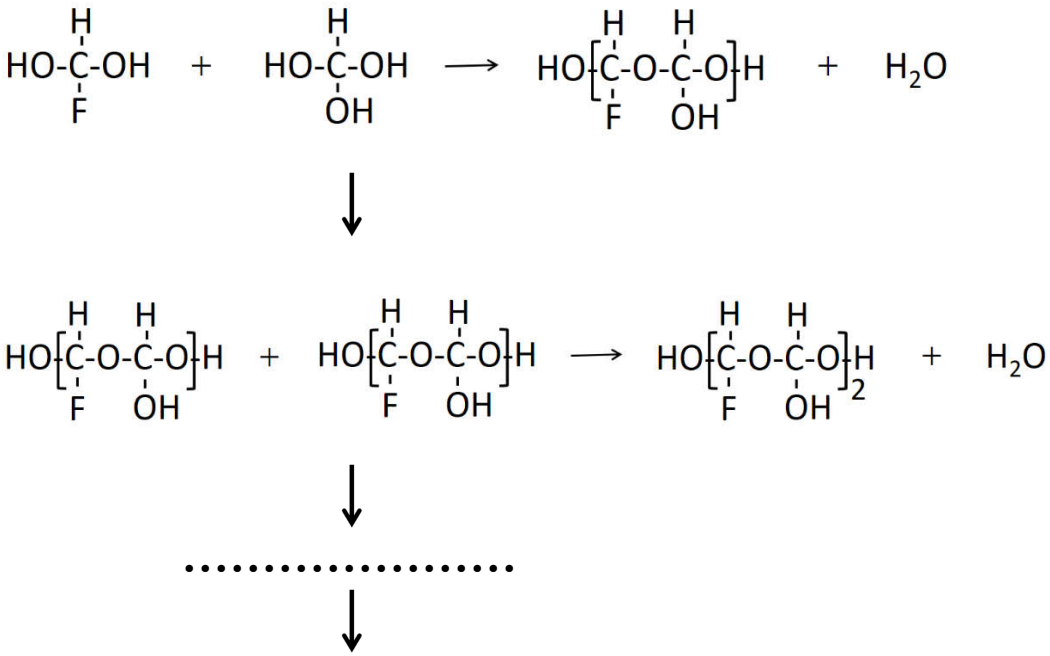

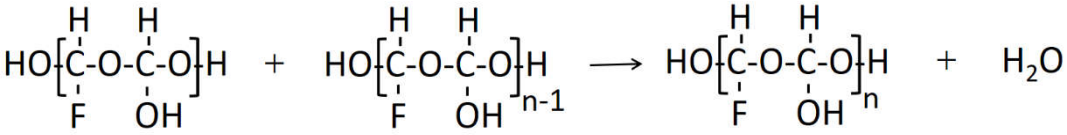

(5) The total reactions may be written as:

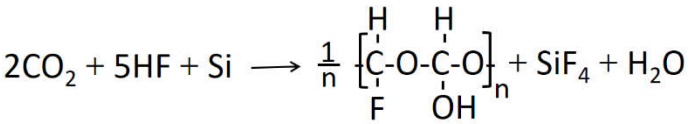

7. Safety notes of fluohydric acid (HF)

HF is a colourless liquid with a pungent, irritating, penetrating odour, which may be fatal if inhaled, absorbed through the skin or swallowed. During the experimental process, we should avoid direct contact and wear chemical protective clothing. HF should be placed in the container made of Teflon. 0.13% benzalkonium chloride (Zephiran®) solution or 2.5% calcium gluconate gel should be prepared to prevent possible injury.

REFERENCE

S1. Azari, M. R., Sadighzadeh, A. and Bayatian, M. (2018). Public health risk management case concerning the city of Isfahan according to a hypothetical release of HF from a chemical plant. Environ Sci Pollut Res. 25, 24704-24712.